

Sizing of Battery Energy Storage System: A Multi-Objective Optimization Approach in DIgSILENT PowerFactory

Wei Hown Tee*^{ID}, Khaldon Ahmed Qaid*^{ID}, Chin Kim Gan*[‡]^{ID}, Joe Siang Keek*^{***}^{ID}, Junainah Sardi*^{ID}

* Faculty of Electrical Engineering, Universiti Teknikal Malaysia Melaka

** Texas Instruments Electronics Malaysia Sdn. Bhd.

(weihowntee@gmail.com, khaldon603@gmail.com, ckgan@utem.edu.my, j-keek@ti.com, junainah@utem.edu.my)

[‡]Corresponding Author; Chin Kim Gan, Faculty of Electrical Engineering, Universiti Teknikal Malaysia Melaka, Jalan Hang Tuah Jaya, 76100 Durian Tunggal, Melaka Tel: +60 62701310, ckgan@utem.edu.my

Received: 19.05.2023 Accepted: 27.06.2023

Abstract- In the paradigm of the increasing trend to prevent global warming, renewable energy sources applications integrated with battery energy storage system (BESS) are gaining attention for reducing the usage of fossil fuels in electrical power generation. In this regard, a multi-objective optimization script in DIgSILENT Programming Language (DPL) which links with software modelling and scripting simulation is developed in this study. Formulation for multiple objectives for optimization of BESS sizing with particle swarm optimization (MOPSO) and load flow simulation are applied in the DPL script. The considered objective functions aim to improve the network performance by reducing power loss, voltage deviations and system costs. Pseudo code of BESS optimal sizing with multi-objective algorithm is presented in this research. The BESS with optimal sizing was discovered for improving the network performance in the tested reference network. The optimal BESS size obtained is 2.94 MW with a system cost of MYR 2404.76. The total energy losses can be reduced by approximately 16% from the base case energy losses with the optimal BESS size. The findings of the research reveal that the BESS sizing with MOPSO is applicable in DPL operations alone to solve power system problems.

Keywords Particle swarm optimization; multi-objective optimization; battery energy storage system; optimal sizing; DIgSILENT PowerFactory.

Nomenclature

Battery energy storage system	BESS
BloombergNEF	BNEF
DIgSILENT Programming Language	DPL
Genetic algorithm	GA
Improve particle swarm optimization	IPSO
Multi-objective optimization	MOO
Multi-objective particle swarm optimization	MOPSO
On-load tap charger	OLTC
Particle swarm optimization	PSO
Photovoltaic and Smart Grid	PVSG
Second order cone program	SOCP
Universiti Teknikal Malaysia Melaka	UTeM

1. Introduction

Countries around the globe are currently facing challenges to reduce the electrical power generation generated by the burning of fossil fuels which contributes to global warming. As a result, the applications of renewable energy sources integrated with grid have received huge attention by researchers nowadays. In the recent BloombergNEF (BNEF) report, around half of the energy demand of the world is projected to be supplied by solar and wind energy by 2050 [1]. On top of that, renewable energy sources are expected to have a dominant power generation mix of almost 50% approaching 2050 [2][3]. However, the unpredicted characteristics of the renewable energy sources will cause instability of the power outputs [4][5]. Hence,

energy storage technologies have emerged as an effective solution for integrating the grid system with renewable energy sources because of their characteristics. Energy storage is widely applied to control the intermittency of renewable energy [6][7][8]. It has been demonstrated that energy storage improves the stability and reliability of renewable energy generation of the network [9][10]. Besides, the ideas have been also applied to both virtual and actual grid system with the benefit of self-consumption of renewable energy generation with storage systems [11][12]. Furthermore, studies showed that energy storage is playing a vital role to provide power quality improvement [13][14][15], frequency and voltage regulation [16][17], energy arbitrage as well as ancillary services [18][19].

At present, researchers show great interest in developing battery energy storage system (BESS) optimization to serve as an integrating option in power systems because of its attributions with rapid reaction. Authors in [20] proposed a second order cone program (SOCP) optimization method based on power flow equations to size the storage. In a study [21], the application of DIgSILENT and MATLAB are used in conjunction with improved particle swarm optimization (IPSO) to solve the voltage fluctuation problem with optimal BESS active power. However, the simulation requires dynamic data exchange file between the software. An optimal BESS control is proposed to reduce excessive on-load tap changer (OLTC) operation caused by renewable energy sources with PSO approach using MATLAB and DIgSILENT software [22]. However, a switch CSV file is needed for data communication between the software. The authors improved the network performance by combining the linkage between MATLAB and DIgSILENT with genetic algorithm (GA) linear programming method to size BESS [23]. However, these studies did not apply both optimization algorithm and loadflow simulation in a single software, for example in DIgSILENT alone.

The studies showed that bio-inspired optimization approaches are widely applied by the researchers due to their flexibility, high accuracy rate and less computational time [24][25]. PSO is one of the established approaches due to its simplicity with coding implementation, short computational time as well as stable convergence properties [26]. It offers a certain appealing feature of good memory where the particles retain the knowledge of good solutions as compared to GA approach [27][28]. PSO is also proven to converge faster and able to escape from being trapped in local optima as compared to Bat algorithm and Tabu search. Moreover, PSO is effective to determine the pareto front in optimizing multi-objective problems [29].

In light of the above, the information of applying multi-objective optimization (MOO) in DIgSILENT DPL script alone is limited. To the best of authors' knowledge, the structure of MOO scripting in DPL has not been reported so far. Hence, the major contributions of this work are

1. To design MOO in programming script to apply both optimization algorithm and loadflow simulation in DIgSILENT without linkage between software.
2. To improve the performance of the distribution network with optimal BESS sizing.

2. Methodology

DIgSILENT PowerFactory is used to apply the methodology developed in this research. Consequently, a series of operations to run the algorithm developed will be carried out in the DPL script. This study is a continuous work from [30], where the algorithm is developed to optimize two objective functions in the DPL script. The DPL script will be used to execute both network model in the simulation interface and script operation in the software at the same time. As a result, the DPL script will interface with the database of the network model object to access, record and perform operation based on the operation functions written in the script.

1.1. Optimization Objectives and Constraints

A multi-objective problem for the BESS sizing of the network is formulated in this study. The first objective function aims to reduce the power loss and voltage deviations of the network with the integration of BESS which can be expressed as

$$\text{Objective Function 1} = \text{optimum}(BESS_{size}) \quad (1)$$

$$\text{optimum}(BESS_{size}) = \left[\frac{\sum_{h=1}^H \sum_{i=1}^N P_{loss_{BESS}}}{\sum_{h=1}^H \sum_{i=1}^N P_{loss_{base}}} \right] + \left[\frac{\sum_{h=1}^H \sum_{i=1}^N (V_{pu}^{BESS}(i))^2}{\sum_{h=1}^H \sum_{i=1}^N (V_{pu}^{base}(i))^2} \right] \quad (2)$$

where $P_{loss_{BESS}}$ is the power loss with BESS in MW, $P_{loss_{base}}$ is the initial power loss without BESS in MW, V_{pu}^{BESS} is the voltage magnitude with BESS in per unit at bus i , V_{pu}^{base} is the base voltage magnitude in per unit, N denotes the total buses number, h denotes the study hours, and H denotes the total number of study hours. This objective function is a linear combination of two performance indices. The denominators in the expressions (2) indicate the sum of real power loss and the sum of the squares of the voltage deviations without the integration of BESS while the numerators are presenting the variables with the integration of BESS [31].

Next, the algorithm aims to reduce the system costs. The equation can be expressed as

$$\text{Objective Function 2} = \min(Cost_{system}) \quad (3)$$

$$\min(Cost_{system}) = Cv + Cl + Cp \quad (4)$$

$$Cv = \left[\sum_{h=1}^H \sum_{i=1}^N |V_i - V_{ref}| \right] \times \varphi_v \quad (5)$$

$$Cl = \sum_{h=1}^H \sum_{i=1}^N |P_{loss_i}| \times \varphi_l \quad (6)$$

$$Cp = \text{Peakload} \times H \times \varphi_p \quad (7)$$

where Cv is voltage regulation charge, Cl is power loss charge, Cp is peak demand charge, V_i is the magnitude of the voltage per unit of the bus, V_{ref} is set as 1 p.u. base voltage reference, φ_v is the cost rate of voltage regulation at 0.63 MYR/ p.u., φ_l is the cost rate of power loss at 1.26 MYR/ kWh and φ_p is the cost rate of peak demand at 2.43 MYR/ kW [32][33]. The objective functions are subjected to the following constraints

$$P_{grid} = \sum_{i=1}^N Load + \sum_{i=1}^N Loss \quad i = 1, 2, \dots, N \quad (8)$$

$$0 \leq LOSS_{BESS} \leq LOSS_{base} \quad (9)$$

$$0 \leq P_{BESS} \leq P_{PV} \quad (10)$$

$$0.95 \leq V_i \leq 1.05 \quad (11)$$

where P_{grid} is the total grid power in MW of the system, $LOSS_{BESS}$ is the power loss with BESS in MW, $LOSS_{base}$ is the base power loss of the system in MW, P_{BESS} is the BESS power in MW, P_{pv} is the peak PV power in MW, V_i is the bus voltage.

1.2. Multi-Objective Algorithm

Particle swarm optimization (PSO) is a heuristic method that was inspired by the birds' behavior. In the algorithm, the particle has its own velocity as well as position property which is able to explore for a possible solution in search space. The velocity of the particle represents the fast or slow movement of the particle, whereas the position of the particle represents the particle's direction. Each particle's velocity can be revised based on its personal and global optimal position. These two properties can be calculated as

$$v_j^{i+1} = \omega v_j^i + c_1 r_1 (P_{best}^i - x_j^i) + c_2 r_2 (G_{best}^i - x_j^i) \quad (12)$$

$$x_j^{i+1} = v_j^{i+1} + x_j^i \quad (13)$$

where ω denotes to the inertia weight of the algorithm, r_1 and r_2 are the values randomly ranged from 0 to 1, c_1 and c_2 are cognitive and social parameters, P_{best}^i and G_{best}^i are personal and global best solution respectively.

The inertia weight of the algorithm influences the velocity and direction of the particle, which brings a big effect on the particle's convergence. According to [34], PSO has a higher convergence speed to achieve local optimum with smaller inertia weight while higher possibility to have global search with greater inertia weight. However, the convergence speed is reduced and the number of iterations increases with greater inertia weight. In this study, the particles initially aim to search globally. After obtaining the swarm particle, the convergence speed increases to obtain the optimum value. Hence, the ω of this study is to decrease between 0.9 to 0.4 and be calculated as

$$\omega = \omega_{high} - (\omega_{high} - \omega_{low}) \times \frac{i}{i_{max}} \quad (14)$$

MOPSO is popularly implemented in optimizing multi-objective problems because of its simple structure, parameter settings as well as fast convergence characteristics [35][36]. MOPSO is relatively complex as compared to PSO in terms of selecting personal and global optimal solutions. It obeys the following principles

1. When the solutions are non-dominated, the best individual position will be randomly selected from one of the particle solutions.

2. Based on the crowding degree in Eq. (15), a leader in the non-dominated solutions is selected as global optimal.

$$CD_i = \frac{|f_1(x_{i+1}) - f_1(x_{i-1})|}{f_1^{max} - f_1^{min}} + \frac{|f_2(x_{i+1}) - f_2(x_{i-1})|}{f_2^{max} - f_2^{min}} \quad (15)$$

The maximum iteration (N_i) in this study is 30, with a population (N_p) of 100. The repository size (N_r) is 50. The learning factors of the algorithm, c_1 and c_2 are set as 0.5 and 0.6. The operation of MOPSO is as follows:

1. Define the objective function constraints and initialize the optimization parameters.
2. Define swarm iteration $i = 1$ with random particle velocity and position.
3. Create grid to store non-dominated solutions.
4. Declare swarm particle $j = 1$.
5. Objective function is executed for the respective particle and iteration.
6. Select leader according to crowding degree. Explore and determine P_{best} and G_{best} of j^{th} particle in i^{th} iteration. If the objective function of j^{th} dominates in j^{th} population, the program stores $P_{best} = f_1(x_j), f_2(x_j)$.
7. Add P_{best} to repository. Determine domination in j^{th} repository.
8. Update grid.
9. Update particle j^{th} by 1. Next, the condition is validated: If particle $j^{\text{th}} + 1 \leq N_p$, go back to Step 5.
10. If P_{best} dominates in j^{th} population, adjust G_{best} of $i^{\text{th}} = P_{best}$ at i^{th} .
11. Plot pareto solutions.
12. Update iteration i^{th} is by 1. Next, the condition is validated: If iteration $i^{\text{th}} + 1 \leq N_i$, go back to Step 4 and the new particle velocity as well as position are updated for $i^{\text{th}} + 1$. Update new inertia weight.
13. If iteration $i^{\text{th}} + 1 \geq N_i$, the algorithm quits the operation and BESS size is acquired.

The flowchart of MOPSO BESS sizing operation between DPL script and DIgSILENT environment is presented in Figure 1. The detailed process of the MOPSO is presented in the Pseudo code, as illustrated in Figure 2.

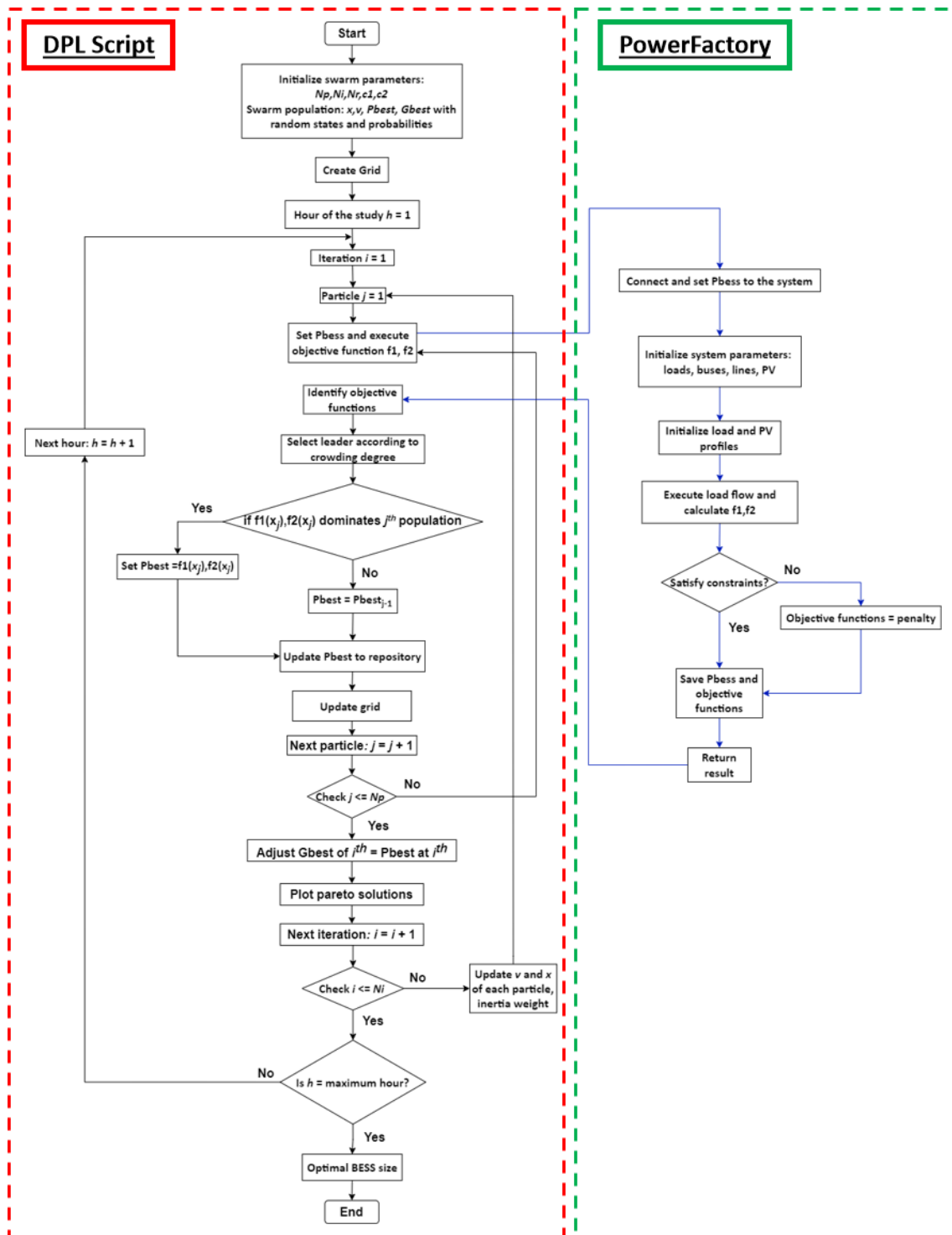


Fig. 1. The flowchart of MOPSO in DigSILENT.

```

Algorithm: Multi-objective particle swarm optimization (MOPSO)
01: Begin, initialize the parameters  $N_i, N_p, N_r, c_1, c_2$ 
02: Initialize DPL object and set of the system  $Gen, Load, Bus, Line, BESS, PV, Ldf$ 
03: Create grid in DPL
04: Execute objective function  $f1, f2$ 
05: Set initial Pbest and Gbest
06: for  $h = 1$  to maximum study hour,  $H$ 
07:     for  $i = 1$  to maximum number of iterations,  $N_i$ 
08:         for  $j = 1$  to maximum number of particles,  $N_p$ 
09:             Update the velocity of the particles  $v_j^{t+1}$  using equation (12)
10:             Update the position of the particles  $x_j^{t+1}$  using equation (13)
11:             Update the inertia weight using equation (14)
12:             Execute loadflow in DIgSILENT PowerFactory
13:             Evaluate the objective functions of the updated position  $f1_{xi}, f2_{xi}$ 
14:             Select leader according to crowding degree using equation (15)
15:             if  $f1_{xi}, f2_{xi}$  satisfy constraints then,
16:                 Save Pbest and  $f1_{xi}, f2_{xi}$ 
17:             else  $f1_{xi}, f2_{xi} = \text{penalty}$ 
18:             end if
19:             Update the personal best by:
20:             if  $f1_{xi}, f2_{xi}$  dominates  $j^{th}$  population then,
21:                  $Pbest = f1_{xi}, f2_{xi}$ 
22:             end if
23:             Update the  $Pbest$  to repository and grid
24:             Update the global best by:
25:             if  $Pbest$  dominates in  $j^{th}$  population then,
26:                  $Gbest = Pbest_i$ 
27:             end if
28:             Update grid and plot pareto
29:         end j
30:     Check stopping criteria, if  $i < N_i$  go to step7 else go to next step.
31: end i
32: Check stopping criteria, if  $h < H$  go to step6 else go to next step.
33: end h
    
```

Fig. 2. The Pseudo code of MOPSO in DIgSILENT.

3. Case Study

The normalized PV and load profiles of the study are presented in Figure 3. The modified urban reference network with 33 & 11 kV feeders of Malaysia as shown in Figure 4 [37] is applied as the test system. The PV and BESS were installed at the end of each feeder. The parameters of the reference network are presented in Table 1. The PV data are collected from the PV system installed at the Research Laboratory of Photovoltaic System and Smart Grid, Universiti Teknikal Malaysia Melaka (UTeM) [7].

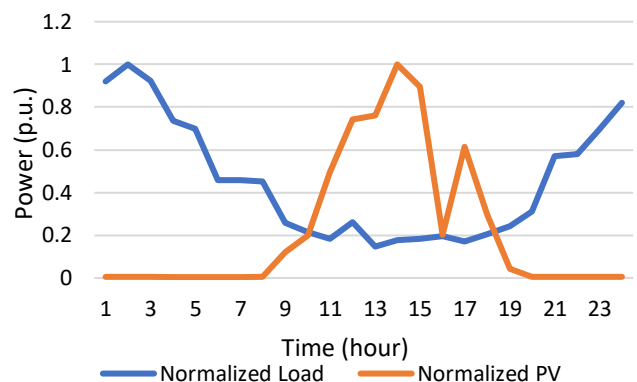


Fig. 3. PV power and load demand profile used in this study.

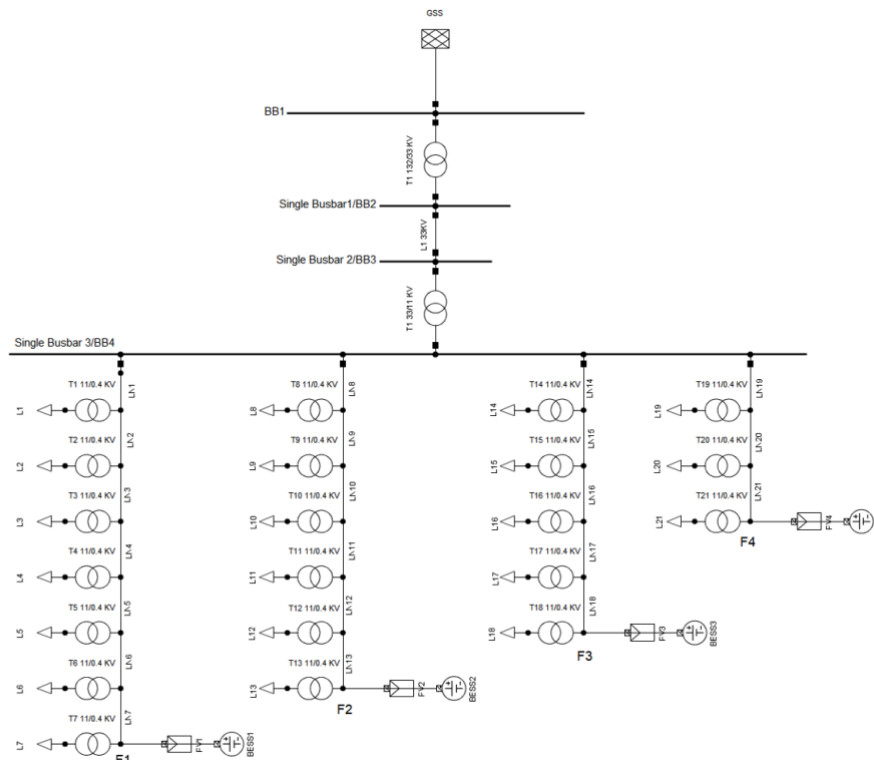


Fig. 4. Urban reference network with 33 & 11 kV feeders.

Table 1. Parameters of urban reference network with 33 & 11 feeders.

Parameters	Average Value			
	F1	F2	F3	F4
PV capacity (MW)	4.00	3.50	3.00	2.50
Maximum load demand (MW)	3.59	3.01	2.77	2.26
<u>Transformer</u>				
33/11 kV capacity (MVA)	30.00			
132/33 kV capacity (MVA)	45.00			
Number of 11/0.4 kV transformers	7.00	6.00	5.00	3.00
11/0.4 kV loading (MVA)	0.58	0.50	0.55	0.76
11/0.4 kV capacity (MVA)	1.00	1.00	1.00	1.00
11/0.4 kV transformer loading (MW)	0.52	0.45	0.50	0.76
<u>Feeder</u>				
33 kV length (km)	4.43			
11 kV length (km)	4.25	2.88	1.70	0.94
Distances between 11/0.4 kV transformers (km)	0.61	0.48	0.34	0.31

4. Results and Discussions

MOPSO is implemented to take into account the BESS sizing with the beneficial objectives of reducing power loss, voltage deviation and system costs. The simulation is conducted in DIgSILENT. The fitness function values and optimal BESS size for F1 feeder are shown in Table 2 with computation time of 4312.02s. Figure 5 presents the pareto optimal front with a variety of leader selections for various objective function 1 (OF1) values correspond to the system costs obtained in the study. The ideal compromise position obtained by the MOPSO is with OF1 value of 3.04 and

objective function 2 (OF2) cost of MYR 2404.76, with optimal BESS solution of 2.94 MW. Besides, boundary solutions can be observed also from the pareto fronts. Firstly, the maximum OF1 can be obtained at 3.12, with the increase of 2.65% from the best compromise solution, followed by MYR 2404.11. Next, the minimum OF1 is with MYR 2406.07, with a reduction percentage of 2.04% from OF1 value of the best compromise solution.

The power losses for the solutions in comparison to the base case are presented in Figure 6. The results reveal that the BESS sizing through MOPSO is able to reduce the power loss of the system. For the base case, the losses are the highest

when there is no PV power (during midnight, and from late evening to 12.00 a.m.) with maximum value of 0.51 MW losses, as well as when PV power is available (from morning until evening) with the maximum value of 0.45 MW losses. This can be explained that the demands are high when the consumers are back from work in the late evening until early morning. Low power usage during the afternoon when PV power is highly available will also lead to power losses because of the excess power generated by PV that flows back to the grid. The optimal solution with 2.94 MW BESS size can reduce the losses of the base case by storing excessive PV power during afternoon hours with low demand, and discharging power to support the load when demand is high during nighttime. The base case has the highest energy losses per day, which is 7.30 MWh, followed by the maximum OF1 (3.29 MW BESS) of 6.22 MWh, optimal solution (2.94 MW BESS) of 6.13 MWh and lastly minimum OF1 (2.94 MW BESS) with 6.04 MWh.

The voltage profile for the base case and optimal solution with respect to BESS power is shown in Figure 7. The BESS improves the voltage profile during high demand hours by discharging power into the network. Moreover, the voltage deviations are reduced with the charging of excess PV power into the BESS during low load demand hours in the afternoon period. Table 3 shows the summary of optimal BESS sizing of MOPSO with F1, F2, F3 and F4. It can be observed that the deployment of BESS at F1 has the highest energy losses reduction as compared to the remaining feeders. This is because F1 feeder has the largest load demand with the

greatest PV capacity. Besides, F1 feeder has the longest 11 kV feeder that contributes to the highest losses among F1 to F4 feeders. Hence, the implementation of optimal BESS size at F1 feeder will have the highest impact on the network performance. Initially, there will be losses in the feeder due to the power transmitted from the main transformer to the end of the feeder. When the PV is connected, the voltage magnitude will increase at the end of the feeder due to the reverse power flow caused by the excess PV power. This issue can be solved by the installation of BESS at the location where BESS can reduce the reverse power flow by charging the excess power generated by PV into the feeder and hence reduce the power losses across the feeder.

Table 2. Solutions of MOPSO obtained for F1.

Item	Minimum OF1	Best Compromise	Maximum OF1
PV size (MW)	4.00	4.00	4.00
BESS size (MW)	2.52	2.94	3.29
OF1 magnitude	2.97	3.04	3.12
System cost (OF2) (MYR)	2406.07	2404.76	2404.11

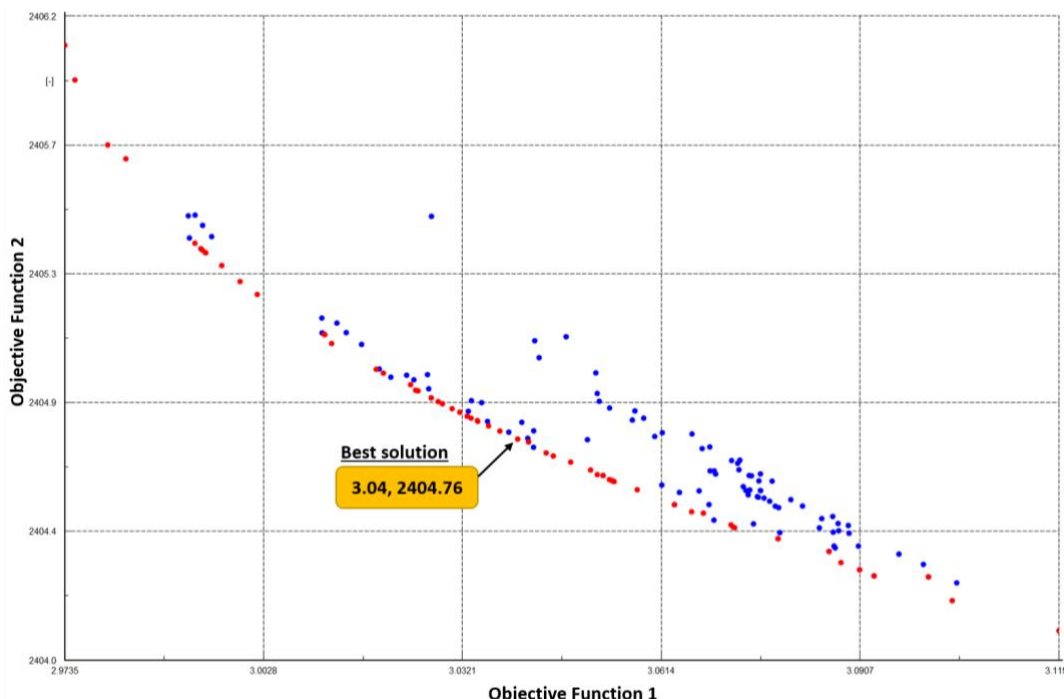


Fig.5. Pareto optimal solutions produced by MOPSO.

Table 3. Summary of optimal BESS sizing in the feeders.

	F1	F2	F3	F4
PV size (MW)	4.00	3.50	3.00	2.50
BESS size (MW)	2.94	2.67	2.05	1.93
OF1 magnitude	3.04	3.01	3.07	2.99
System cost (OF2) (MYR)	2404.76	2343.3	2286.24	2250.33
Energy losses reduction (MWh)	6.13	5.98	5.47	5.21

By taking into account the network performance, it is also demonstrated that the overall improved voltage profile in one day is sustained within the operating voltage, with reduced power losses by implementing the optimal sizing of BESS through MOPSO. This enhances the power quality and improves the reliability of the network. The MOPSO shown in this study can offer optimal BESS sizing integrated with PV in the distribution network as well as benefit in terms of cost. Moreover, it can also be effectively deployed to other real networks connected to grid systems with more updated problem formulation or objectives to optimize the BESS size based on the idea and Pseudo code provided in this study.

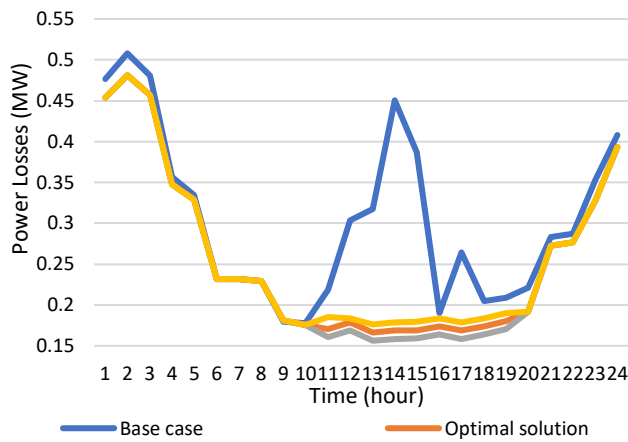


Fig. 6. Power losses comparison of the solutions.

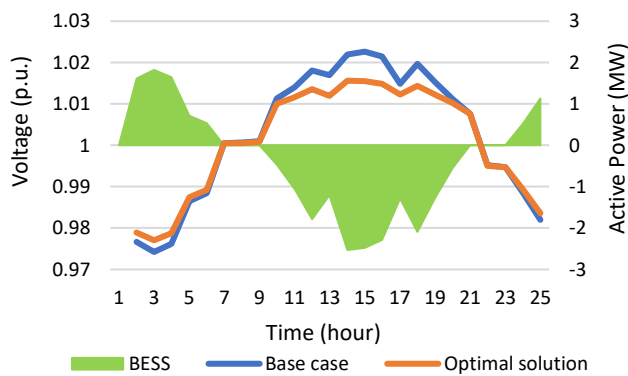


Fig. 7. Voltage profiles that correspond to BESS power.

5. Conclusion

This study presented optimal BESS sizing with MOPSO in the DPL script of DIGSILENT PowerFactory. The developed MOPSO reduced the total power losses, improved the voltage profile as well as the costs associated with the distribution network. In the MOPSO, various candidate solutions of OF1 and OF2 are acquired with optimal BESS size through the pareto optimal front. The best solution identified is OF1 value of 3.04 and OF2 of MYR 2404.76 with optimal BESS size of 2.94 MW. Besides, the optimal BESS size can reduce the total energy losses by 6.13 MWh, which is approximately 16% reduction from 7.30 MWh. The findings reveal that the network has enhanced voltage profile with BESS deployment, resulting in more system costs that can be saved. However, it is noted that this work does not consider the smoothing of solar PV output with optimal BESS sizing. Hence, the future potential of this study consists of the development of objective functions in MOPSO that focus on the limitation of renewable energy intermittency, the impact of BESS applications and techno-economic areas.

Acknowledgements

The authors gratefully acknowledge the support given by Universiti Teknikal Malaysia Melaka (UTeM) for this work.

References

- [1] “Bloomberg New Energy Outlook 2019: The future of the energy sector - Power Technology.” [Online]. Available: <https://www.power.technology.com/news/bloomberg-new-energyoutlook-2019-2/> (accessed Jul. 22, 2022).
- [2] A. A. Kebede, T. Kalogiannis, J. Van Mierlo, and M. Bercibar, “A comprehensive review of stationary energy storage devices for large scale renewable energy sources grid integration,” *Renew. Sustain. Energy Rev.*, vol. 159, p. 112213, 2022.
- [3] V. Henze, “Energy Storage Is a \$620 Billion Investment Opportunity to 2040 | BloombergNEF,” BloombergNEF, 6 Nov. 2018, [about.bnef.com/blog/energy-storage-620-billion-investment-opportunity-2040.](https://about.bnef.com/blog/energy-storage-620-billion-investment-opportunity-2040/), 2018. <https://about.bnef.com/blog/energy-storage-620-billion-investment-opportunity-2040/> (accessed Nov. 26, 2021).
- [4] W. Wang, B. Yuan, Q. Sun, and R. Wennersten, “Application of energy storage in integrated energy systems—A solution to fluctuation and uncertainty of renewable energy,” *J. Energy Storage*, vol. 52, p. 104812, 2022.
- [5] H. Shahinzadeh, J. Moradi, W. Yaïci, M. Longo, and Z. Azani, “Impacts of Energy Storage Facilities on Resilient Operation of Multi-Carrier Energy Hub Systems,” in *2022 10th International Conference on Smart Grid (icSmartGrid)*, pp. 339–344, 2022.
- [6] J. Dey, N. Mohammad, and M. T. Islam, “Analysis of

- a Microgrid having Solar System with Maximum Power Point Tracking and Battery Energy System,” in *2022 10th International Conference on Smart Grid (icSmartGrid)*, pp. 179–184, 2022.
- [7] W. H. Tee, C. Kim Gan, J. B. Sardi, K. Azmi Baharin, and K. K. Kong, “Probabilistic sizing of battery energy storage system for solar photovoltaic output smoothing,” *PECon 2020 IEEE Int. Conf. Power Energy*, pp. 350-355, 2020.
- [8] M. A. Pinazo and J. L. R. Martinez, “Intermittent power control in wind turbines integrated into a hybrid energy storage system based on a new state-of-charge management algorithm,” *J. Energy Storage*, vol. 54, p. 105223, 2022.
- [9] L. A. Wong, V. K. Ramachandaramurthy, P. Taylor, J. B. Ekanayake, S. L. Walker, and S. Padmanaban, “Review on the optimal placement, sizing and control of an energy storage system in the distribution network,” *J. Energy Storage*, vol. 21, pp. 489–504, 2019.
- [10] D. Al kez, A. M. Foley, N. McIlwaine, D. J. Morrow, B. P. Hayes, M. A. Zehir, L. Mehigan, B. Papari, C. S. Edrington, and M. Baran, “A critical evaluation of grid stability and codes, energy storage and smart loads in power systems with wind generation,” *Energy*, vol. 205, p. 117671, 2020.
- [11] M. Shamshiri, C. K. Gan, J. Sardi, M. T. Au, and W. H. Tee, “Design of Battery Storage System for Malaysia Low Voltage Distribution Network with the Presence of Residential Solar Photovoltaic System,” *Energies*, vol. 13, p. 4887, 2020.
- [12] J. Sardi, N. Mithulananthan, M. M. Islam, and C. K. Gan, “Framework of virtual microgrids formation using community energy storage in residential networks with rooftop photovoltaic units,” *J. Energy Storage*, vol. 35, p. 102250, 2021.
- [13] Y. Iwasaki, “Dynamic Switching Method with Energy Storage Devices in Wind Power Generation,” in *2022 10th International Conference on Smart Grid (icSmartGrid)*, pp. 165–168, 2022.
- [14] M. Sarr, M. Thiam, B. Niang, O. Ba, and L. Thiaw, “BESS deployment and Virtual Power Plant: Technical and financial analysis of the Senelec network to assess the relevance,” in *2022 10th International Conference on Smart Grid (icSmartGrid)*, pp. 118–123, 2022.
- [15] S. Hajiaghahi, A. Salemnia, and M. Hamzeh, “Hybrid energy storage system for microgrids applications: A review,” *J. Energy Storage*, vol. 21, pp. 543–570, 2019.
- [16] U. Akram, M. Nadarajah, R. Shah, and F. Milano, “A review on rapid responsive energy storage technologies for frequency regulation in modern power systems,” *Renew. Sustain. Energy Rev.*, vol. 120, p. 109626, 2020.
- [17] N. McIlwaine, A. M. Foley, D. J. Morrow, D. Al Kez, C. Zhang, X. Lu, and R. J. Best, “A state-of-the-art techno-economic review of distributed and embedded energy storage for energy systems,” *Energy*, vol. 229, p. 120461, 2021.
- [18] E. Pusceddu, B. Zakeri, and G. C. Gissey, “Synergies between energy arbitrage and fast frequency response for battery energy storage systems,” *Appl. Energy*, vol. 283, p. 116274, 2021.
- [19] K. Oureilidis *et al.*, “Ancillary services market design in distribution networks: Review and identification of barriers,” *Energies*, vol. 13, no. 4, p. 917, 2020.
- [20] E. Grover-Silva, R. Girard, and G. Kariniotakis, “Optimal sizing and placement of distribution grid connected battery systems through an SOCP optimal power flow algorithm,” *Appl. Energy*, vol. 219, pp. 385–393, 2018.
- [21] K. Tantrapon, P. Jirapong, and P. Thararak, “Mitigating microgrid voltage fluctuation using battery energy storage system with improved particle swarm optimization,” *Energy Reports*, vol. 6, pp. 724–730, 2020.
- [22] T. Akapan, P. Thararak, and P. Jirapong, “Optimal real-time operation of battery energy storage systems for reducing on-load tap changer operation of substation transformers,” in *AIP Conference Proceedings*, vol. 2681, no. 1, p. 20033, 2022.
- [23] M. R. Jannesar, A. Sedighi, M. Savaghebi, and J. M. Guerrero, “Optimal placement, sizing, and daily charge/discharge of battery energy storage in low voltage distribution network with high photovoltaic penetration,” *Appl. Energy*, vol. 226, pp. 957–966, 2018.
- [24] M. A. Hannan, S. B. Wali, P. J. Ker, M. S. Abd Rahman, M. Mansor, V. K. Ramachandaramurthy, K. M. Muttaqi, T. M. I. Mahlia, and Z. Y. Dong, “Battery energy-storage system: A review of technologies, optimization objectives, constraints, approaches, and outstanding issues,” *J. Energy Storage*, vol. 42, p. 103023, 2021.
- [25] R. Raghu, M. Sankaraiah, R. S. S. Nuvvula, and M. Venkatesh, “Dispatchable and Non-dispatchable Distributed Generation Reactive Power Coordination with Reactive Power-controlled Devices using Grey Wolf Optimizer,” in *11th International Conference on Renewable Energy Research and Application (ICRERA)*, 2022, pp. 33–41, 2022.
- [26] M. H. K. Roni, M. S. Rana, H. R. Pota, M. M. Hasan, and M. S. Hussain, “Recent trends in bio-inspired meta-heuristic optimization techniques in control applications for electrical systems: A review,” *Int. J. Dyn. Control*, pp. 1–13, 2022.
- [27] T. A. Jumani, M. W. Mustafa, A. S. Alghamdi, M. M. Rasid, A. Alamgir, and A. B. Awan, “Swarm intelligence-based optimization techniques for dynamic response and power quality enhancement of

- AC microgrids: A comprehensive review,” *IEEE Access*, vol. 8, pp. 75986–76001, 2020.
- [28] T. O. Ajewole, O. Oladepo, K. A. Hassan, A. A. Olawuyi, and O. Onarinde, “Comparative Study of the Performances of Three Metaheuristic Algorithms in Sizing Hybrid-Source Power System,” *Turkish Journal of Electrical Power and Energy Systems*, vol. 2, no. 2, pp. 134-146, 2022.
- [29] Q. Gu, Q. Wang, X. Li, and X. Li, “A surrogate-assisted multi-objective particle swarm optimization of expensive constrained combinatorial optimization problems,” *Knowledge-Based Syst.*, vol. 223, p. 107049, 2021.
- [30] W. H. Tee, K. A. Qaid, C. K. Gan, and P. H. Tan, “Battery Energy Storage System Sizing Using PSO Algorithm in DIGSILENT PowerFactory,” *Int. J. Renew. Energy Res.*, vol. 12, no. 4, pp. 2143–2151, 2022.
- [31] B. Mukhopadhyay and D. Das, “Multi-objective dynamic and static reconfiguration with optimized allocation of PV-DG and battery energy storage system,” *Renew. Sustain. energy Rev.*, vol. 124, p. 109777, 2020.
- [32] P. Boonluk, S. Khunkitti, P. Fuangfoo, and A. Siritaratiwat, “Optimal siting and sizing of battery energy storage: Case study seventh feeder at Nakhon Phanom substation in Thailand,” *Energies*, vol. 14, no. 5, p. 1458, 2021.
- [33] N. Jayasekara, M. A. S. Masoum, and P. J. Wolfs, “Optimal operation of distributed energy storage systems to improve distribution network load and generation hosting capability,” *IEEE Trans. Sustain. Energy*, vol. 7, no. 1, pp. 250–261, 2015.
- [34] B. Sun, “A multi-objective optimization model for fast electric vehicle charging stations with wind, PV power and energy storage,” *J. Clean. Prod.*, vol. 288, p. 125564, 2021.
- [35] M. Kharrich, O. H. Mohammed, N. Alshammari, and M. Akherraz, “Multi-objective optimization and the effect of the economic factors on the design of the microgrid hybrid system,” *Sustain. Cities Soc.*, vol. 65, p. 102646, 2021.
- [36] C. A. C. Coello, G. T. Pulido, and M. S. Lechuga, “Handling multiple objectives with particle swarm optimization,” *IEEE Trans. Evol. Comput.*, vol. 8, no. 3, pp. 256–279, 2004.
- [37] H. Salah Mohammed, C. Kim Gan, and M. R. Ab Ghani, “Technical impacts of solar photovoltaic systems integration into Malaysian medium voltage reference networks,” *Int. J. Nonlinear Anal. Appl.*, vol. 11, pp. 265–276, 2020.